Chinese Journal of
POLYMER SCIENCE

RESEARCH ARTICLE

https://doi.org/10.1007/s10118-025-3408-5
Chinese J. Polym. Sci. **2025**, *43*, 1825–1836

Synthesis and Characterization of Terpenoid-derived Poly(6,10-dimethyl-1,3,9-undecatriene): A Biobased and Sustainable Polymer from Renewable Citronellal

Xin Li, Feng Wang, Qi Yang*, Xue-Quan Zhang, and Heng Liu*

Shandong Provincial College Laboratory of Rubber Material and Engineering/ Key Laboratory of Rubber-Plastics, Ministry of Education, Qingdao University of Science & Technology, Qingdao 266042, China

Electronic Supplementary Information

Abstract As a naturally occurring terpenoid that is abundant in essential oils, citronellal remains largely unexplored in polymer science. Herein, we present a novel strategy for converting bio-based citronellal into the diene monomer 6,10-dimethyl-1,3,9-undecatriene (DMUT), which undergoes neodymium-catalyzed coordination polymerization to yield poly(6,10-dimethyl-1,3,9-undecatriene) (PDMUT), a bio-derived polydiene polymer. This provides a facile and sustainable route for transforming renewable citronellal into functional polymers. The effects of polymerization conditions on the catalytic performance and polymer characteristics, including molecular weight, polydispersity, and microstructure, were systematically investigated. In addition, DMUT was successfully copolymerized with isoprene (IP) and 1,3-butadiene (BD), yielding copolymers with tunable compositions and microstructures. These results demonstrate the versatility of DMUT as a renewable building block for both homopolymers and copolymers, paving the way toward bio-based elastomeric materials with customizable properties.

Keywords Citronellal; Polydiene; Coordination homo/copolymerization; Bio-based

Citation: Li, X.; Wang, F.; Yang, Q.; Zhang, X. Q.; Liu, H. Synthesis and characterization of terpenoid-derived poly(6,10-dimethyl-1,3,9-undecatriene): a biobased and sustainable polymer from renewable citronellal. *Chinese J. Polym. Sci.* **2025**, *43*, 1825–1836.

INTRODUCTION

The modern chemical industry relies heavily on the utilization of fossil resources, with petroleum playing a pivotal role owing to its extensive application in transportation fuels, combustible oils, and as a raw material for a myriad of chemical products. However, in recent years, growing evidence has indicated that the extensive use of petroleum derivatives is a primary driver of the escalating levels of CO_2 and other atmospheric pollutants, which in turn exacerbates the greenhouse effect. Therefore, the quest for biodegradable, bio-derived, and sustainable alternatives has emerged as a critical area of research in both academia and industry, with the goal of reducing or at least curtailing reliance on fossil resources.[1–4]

Among the diverse compounds derived from biomass, terpene and terpenoid compounds, which are abundant in plants and insects, have recently gained increasing attention over recent decades.[5,6] Beyond their essential roles in flavoring, fragrance, cosmetics, pharmaceuticals, and insect repellents, these compounds have emerged as vital building blocks for the synthesis of polymer materials, including polyketones, polyesters, polyamides, and polydienes, *etc*., showcasing their versatility and potential in the development of sustainable materials.[7–11] In the realm of polydiene, various terpene monomers, like *β*-myrcene,[12–22] *β*-ocimene,[23–27] *β*-farnesene,[28–33] 4,8-dimethyl-1,3,7-nonatriene,[34] alloocimene,[35–38] *etc*., have been polymerized by anionic, radical, coordination polymerization strategies, to give polyterpene elastomers to substitute petroleum-based polybutadiene or polyisoprene synthetic rubbers (Scheme 1). Citronellal is a naturally occurring terpenoid that is primarily found in the essential oils of various plants, such as citronellal (Cymbopogon nardus) and lemon grass (Cymbopogon citratus).[39,40] Besides, Citronellal can also be prepared *via* selective hydrogenation from another important biomass, citral, whose global capacity is up to 63,000 metric tons annually.[41] Citronellal is widely known for its distinct lemon-like odor and has a range of industrial, pharmaceutical, and cosmetic applications, including flavoring agents, fragrances, and insect repellents, *etc*. However, their application in polymer materials remains largely underexplored. Typically present as a racemic mixture of the two isomers, (+/–)-3,7-dimethyloct-6-enal, which features a monoterpenoid aldehydic component that can easily react and transform into other functionalities. Herein, by using the Wittig reaction, the aldehyde functionality

* Corresponding authors, E-mail: qyang@qust.edu.cn (Q. Y.)
E-mail: hengliu@qust.edu.cn (H. L.)

Received May 20, 2025; Accepted June 30, 2025; Published online September 10, 2025

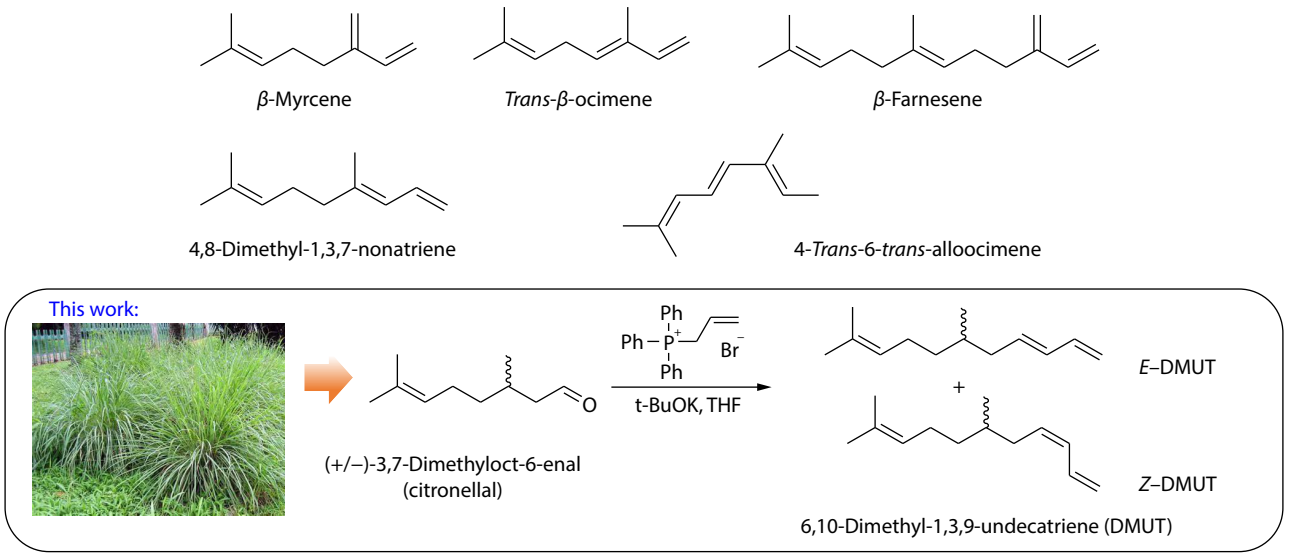

Scheme 1 Representative examples of terpene molecules (top); synthetic procedure of converting terpenioid of Citronellal into polymerizable DMUT (bottom).

was converted into a conjugated diene structure, 6,10-dimethyl-1,3,9-undecatriene (DMUT) (Scheme 1), which was subsequently polymerized by a neodymium (Nd)-based Ziegler-Natta catalyst, a system that exhibits high activity toward substituted diene monomers.[42–48] The influence of polymerization conditions on the properties of the obtained poly(6,10-dimethyl-1,3,9-undecatriene) (PDMUT) products, as well as a detailed structural analysis of PDMUT, were carried out. Moreover, to further assess the structural versatility and potential application scope of DMUT, we extended our investigation to its copolymerization with the conventional diene monomers isoprene (IP) and 1,3-butadiene (BD). The successful incorporation of DMUT into the IP/BD backbones enabled the preparation of bio-based copolymers with adjustable compositions, offering new opportunities for the development of sustainable elastomeric materials. To the best of our knowledge, this is the first report detailing the conversion of citronellal to homo- and copolymeric polydiene materials.

EXPERIMENTAL

Materials

Citronellall and allyltriphenylphosphonium bromide were purchased from HEOWNS (Tokyo, Japan). Potassium *t*-butoxide was provided by Energy Chemical and was used as received. THF was obtained from Fuyu Chemical and distilled with CaH_2 before use. Neodymium neodecanoate (NdV) was purchased from Energy Chemical and diluted to 0.3 mol/L by hexane before use. Diisobutylaluminum hydride (DIBAH, Al(*i*-Bu)$_2$H) was the commercial product of Akzo Nobel and diluted with hexane to a 2.0 mol/L solution before use. Dichlorodimethylsilane (Me_2SiCl_2) and other chloride donors were obtained from Alfa and diluted with toluene solution to 1.0 mol/L.

Analytical Method

The number-average molecular weight (M_n) and molecular weight distribution (M_w/M_n) of polymers were measured at 40 °C using gel permeation chromatography (GPC) equipped with a Waters 515 HPLC pump, four columns (HMW 7 THF, HMW 6E THF×2, HMW 2 THF), and a Waters 2414 refractive index detector. Tetrahydrofuran (THF) was used as eluent at a flow rate of 1.0 mL/min. Sample solutions were filtered through a 0.45 μm microfilter before injection. The values of M_n and M_w/M_n were calculated using polystyrene (PS) calibration. The column was calibrated with monodisperse polystyrene (PS) standards having the Mark-Houwink constants K=1.05×10^{-4}, α=0.731 for PS, K=2.46×10^{-4}, α=0.732 for polybutadiene, and K=4.51×10^{-4}, α=0.66 for polyisoprene. NMR spectra of the samples were recorded on a BRUKER AVANCE NEO 400 MHz spectrometer using $CDCl_3$ as the solvent at ambient temperature and tetramethylsilane (TMS) as an internal standard. MALDI-TOF MS analysis was conducted on a Bruker Microflex LRF mass spectrometer using 2-[(2*E*)-3-(4-*tert*-butylphenyl)-2-methyl-2-propenylidene] malononitrile (DCTB) as the matrix and silver trifluoroacetate as the dopant. The polymer samples were subjected to thermal analysis to assess their degradation characteristics before and after hydrogenation. Thermogravimetric analysis (TGA) was performed using a Discovery TG209F1-LIBRA TGA instrument (NETZSCH). Samples weighing between 5 and 10 mg were placed in platinum pans and analyzed from 20 °C to 800 °C under a nitrogen flow at a heating rate of 10 °C/min. Differential scanning calorimetry (DSC) was performed using a DSC204F1 instrument. The polymer samples were first cooled from room temperature to –80 °C to eliminate any thermal history, then heated to 20 °C. This process was repeated to determine the glass transition temperature (T_g) accurately. A heating rate of 10 °C/min was used for both cycles.

Synthesis of 6,10-Dimethylundeca-1,3,9-triene (DMUT)

To a 200 mL oven dried Schlenk flask was added 14.9 g of allyltriphenylphosphonium bromide (1.2 equiv., 38.9 mmol) and 4.4 g of potassium *t*-butoxide (1.2 equiv., 38.9 mmol), afterwards, 100 mL of THF was added and the flask were filled with N_2. The obtained suspension was cooled to 0 °C and left to be stirred for 15 min. The reaction mixture was then added dropwise to 5 g

https://doi.org/10.1007/s10118-025-3408-5

Citronellal (1.0 equiv., 32.4 mmol) in 15mL of THF. After the reaction continued at 0 ℃ for 1 h, the mixture was slowly warmed to room temperature and stirred for 16 h. A saturated solution of NH_4Cl (20mL) was added. To quench the reaction, the combined organic phases were washed with brine and dried over $MgSO_4$ and the solvent was removed under reduced pressure. The target product was obtained by silica gel chromatograph to give the target product. Yield: 3.25 g, 56%. *Z*:*E* = 53:47. For Z isomer: ^{1}H-NMR (400MHz, $CDCl_3$, δ): 6.64 (m, 1H), 6.04 (m, 1H), 5.47 (m, 1H), 5.20 (d, 1H), 5.13 (m, 2H), 1.97 (m, 4H), 1.68 (s, 3H), 1.60 (s, 3H), 1.51 (m, 1H), 1.36 (m, 1H), 1.16 (m, 1H), 0.89 (dd, 3H). ^{13}C-NMR (400MHz, $CDCl_3$, δ): 131.43; 131.22; 129.97; 129.07; 123.80, 115.66; 35.75; 33.89; 32.11; 24.68; 18.45; 16.58; For *E* isomer: ^{1}H-NMR (400MHz, $CDCl_3$, δ): 6.31 (m, 1H), 6.04 (m, 1H), 5.68 (m, 1H), 4.96 (d, 1H), 5.13 (m, 2H), 2.17 (m, 1H), 1.97 (m, 1H), 1.68 (s, 3H), 1.60 (s, 3H), 1.51 (m, 1H), 1.36 (m, 1H), 1.16 (m, 1H), 0.89 (dd, 3H). ^{13}C-NMR (400MHz, $CDCl_3$, δ): 136.31; 132.83; 130.38; 129.97; 123.80; 113.53; 39.03; 33.89; 31.79; 24.68; 18.45; 16.58. EI-MS for $C_{13}H_{22}$ (*m*/*z*): 201.16 ($M + Na^+$).

General Procedure for 6,10-Dimethylundeca-1,3,9-triene Polymerization

All manipulations were conducted in a dry nitrogen atmosphere. A detailed description of the polymerization procedure is provided below.

Catalyst aging: an ampoule was charged sequentially with $Nd(vers)_3$, DMUT, $Al(i\text{-}Bu)_2H$ (DIBAH) in a designed ratio, and the reaction mixture was left to age at 50 ℃ for 20 min, after which Me_2SiCl_2 was added, and the reaction solution was continued for another 30 min, which eventually gave a yellowish-green solution as the final catalyst solution.

Polymerization process: into an oxygen and moisture-free ampoule that is capped with a rubber septum was added 0.6 mL of DMUT in hexane, and the aged catalyst solution was added. Then the Polymerization was carried out at 50 ℃ for 4 h. To quench the polymerization, 2.0 mL of acidified ethanol containing 2,6-di-*tert*-butyl-4-methylphenol (1 wt%) as a stabilizer was added. The polymer was subsequently washed repeatedly with ethanol and then dried under vacuum at 50 ℃ until it reached a constant weight. The polymer yield was determined using gravimetry.

The DMUT/IP and DMUT/BD copolymerization processes follow the above procedures.

Hydrogenation of PDMUT

PDMUT (0.2 g, 4.4 mmol (C═C)) and *p*-toluenesulfonylhydrazide (1.5 equiv., 6.6 mmol) were added to a dried three-necked flask. Then, 10 ml xylene was added. The reaction mixture was first purged with nitrogen for 10 minutes, and then refluxed at 140 ℃ for 7 h, during which the reaction mixture changed from a white suspension to a pale yellow transparent solution. After the reaction, the solution was poured into excess ethanol to precipitate the hydrogenated product. The solid product was filtered, washed several times with ethanol, and finally dried under vacuum at 40 ℃ to a constant weight. The product yield was > 80%.

RESULTS AND DISCUSSION

Synthesis and Characterization of DMUT

Wittig reaction is a well-established method for transforming carbonyl compounds into alkenes. Reacting Citronellal with phosphorus ylide, which was prepared *in situ* between allyltriphenylphosphonium bromide and potassium t-butoxide (t-BuOK) in tetrahydrofuran (THF), could easily convert aldehyde into a diene functionality to afford 6,10-dimethyl-1,3,9-undecatriene (DMUT) in 56% yield. The chemical structure and purity of DMUT were confirmed by ^{1}H, ^{13}C, and H-H COSY NMR spectroscopy (Fig. 1). As shown in Fig. 1(A), DMUT exists as a mixture of *E*- and *Z*-isomers with an approximate *E*/*Z* ratio of 47:53. For *E*-DMUT isomer, the olefinic protons are observed at δ = 6.31 (H2), 6.07 (H3), 5.70 (H4), 5.08 (H10 and H1b), 4.96 (H1a) respectively (^{13}C: 113.58 (Ca), 132.76 (Cb), 130.46 (Cc), 136.38 (Cd), 123.79 (Cj), 130.05 (Ck)), and clear correlations between H4 and H3, H3 and H2, H2 and H1b, H2 and H1a were identified in the H-H COSY spectrum.[49] For *Z*- isomer, the olefinic protons are observed at δ = 6.63 (H2′), 6.05 (H3′), 5.45 (H4′), 5.09 (H10′ and H1b′), 5.05 (H1a′) respectively (^{13}C: 115.54 (Ca′), 131.16 (Cb′), 129.01 (Cc′), 131.42 (Cd′), 123.79 (Cj′), 130.05 (Ck′)), and similar correlations between H4′ and H3′, H3′ and H2′, H2′ and H1b′, H2′ and H1a′ were also clearly observed.[50] These results confirmed the successful synthesis of DMUT and the coexistence of the two geometric isomers.

Nd-mediated Coordination Polymerization Performances of DMUT

In this study, a typical ternary Nd-based catalytic system consisting of neodymium versatate/diisobutyl aluminum hydride/Me_2SiCl_2 (NdV/DIBAH/Me_2SiCl_2) was utilized to catalyze DMUT polymerization. The investigation commenced by evaluating the influence of the [DIBAH]/[Nd] molar ratio on the overall performance. As shown in Table 1, DMUT was successfully polymerized by the NdV/DIBAH/Me_2SiCl_2 system under the conditions of [DIBAH]/[Nd] = 10–50. Increasing the [DIBAH]/[Nd] ratio from 10 to 50 had minimal effect on the overall catalytic activity, giving poly(6,10-dimethyl-1,3,9-undecatriene) (PDMUT) in moderate yields with smaller changes ranging from 48.8% to 56.3%. Nevertheless, the molecular weights and polydispersities of the obtained PMDUTs were highly sensitive to the [DIBAH]/[Nd] ratios. As the [DIBAH]/[Nd] ratio increased from 10 to 50, the molecular weights gradually decreased from 4.26×10^3 g/mol to 1.76×10^3 g/mol, and the polydispersities narrowed from 1.84 to 1.24. This trend was likely attributed to facilitated reversible chain transfer reactions, a phenomenon commonly observed in the Nd-mediated polymerization of 1,3-butadiene and isoprene monomers.[51,52] Fig. 2(a) illustrates the GPC profiles for PDMUTs obtained from Table 1; at low [DIBAH]/[Nd] ratios, bimodal distributions were first observed, suggesting incomplete activation of the NdV precatalyst under such low DIBAH amounts, which was presumed to generate ill-defined multi-site active species. By gradually increasing the [DIBAH]/[Nd] ratio, NdV could be fully activated, which could lead to unimodal distributed products.

Additionally, the effect of chloride donors, another critical component of the ternary Nd-based catalytic system, on the overall catalytic performance was evaluated. As summarized in Table S1 (in the electronic supplementary information, ESI), varying the chloride donors—Me_2SiCl_2, $CHCl_3$, $AlEt_2Cl$, and $Al_2Et_3Cl_3$—had minimal impact on the activities, giving PDMUT in yields of 52.2%–58.4%. Nevertheless, they significantly influenced the molecular weights and polydispersities

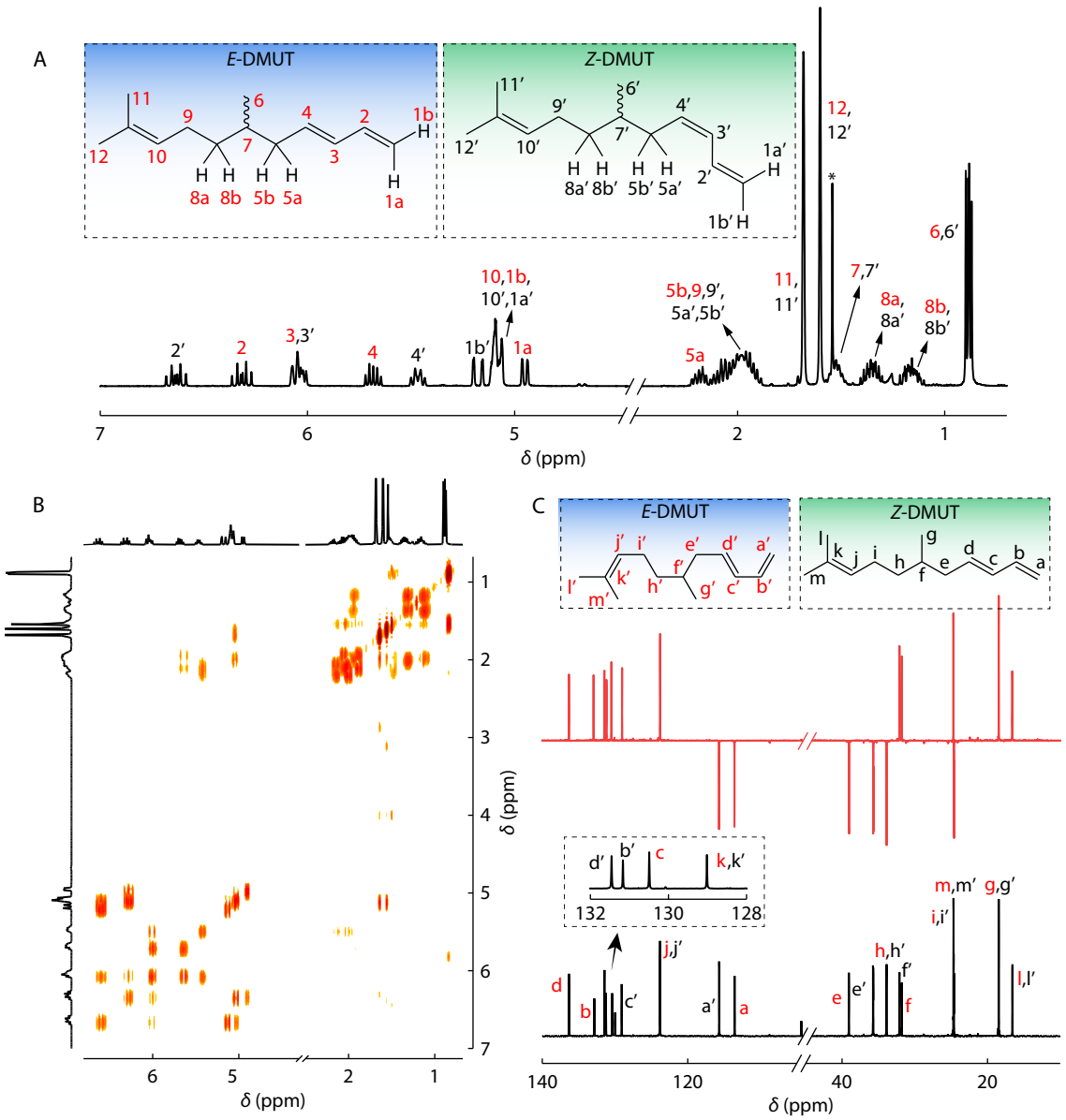

Fig. 1 (A) ^{1}H-NMR, (B) H-H COSY-NMR, (C) ^{13}C-NMR and DEPT 135 spectra of DMUT.

Table 1 Nd-promoted DMUT polymerization under different [DIBAH]/[Nd] ratios.

Run	[DIBAH]/[Nd] (mol/mol)	Yield (%)	M_n [a] (×10^3)	M_w [a] (×10^3)	PDI [a]	Microstructure [b] (%)	
						1,4-	1,2-
1	10	48.8	4.26	7.82	1.84	17.95	82.05
2	20	51.9	2.87	4.66	1.67	24.67	75.33
3	25	54.2	2.30	3.79	1.65	25.77	74.23
4	30	52.6	2.02	2.87	1.42	26.88	73.12
5	40	53.2	1.78	2.39	1.34	27.47	72.53
6	50	56.3	1.76	2.19	1.24	28.08	71.92

Polymerization conditions: [DMUT]=1.85 mol/L, in hexane, 50 °C, 24 h. [M]/[Nd]=500, Cl/Nd=3.0 (Me_2SiCl_2). [a] Determined by GPC, using polystyrene as standard. [b] Determined by NMR.

of the PDMUTs, as shown in Fig. 2(b), with $CHCl_3$ and Me_2SiCl_2 giving the smallest and highest molecular weights of 1.02×10^3 and 1.78×10^3 g/mol, respectively.

By varying the [DMUT]/[Nd] ratio, the molecular weights of PDMUT could be tuned over a broader range (Fig. 2c). As shown in Table 2, increasing the [DMUT]/[Nd] ratio from 200 to 2000 led to a monotonic increase in molecular weight, ranging from 1.49×10^3 g/mol to 4.24×10^3 g/mol. Further increase in the molecular weight of PDMUT is fundamentally constrained by the steric hindrance inherent to the DMUT

https://doi.org/10.1007/s10118-025-3408-5

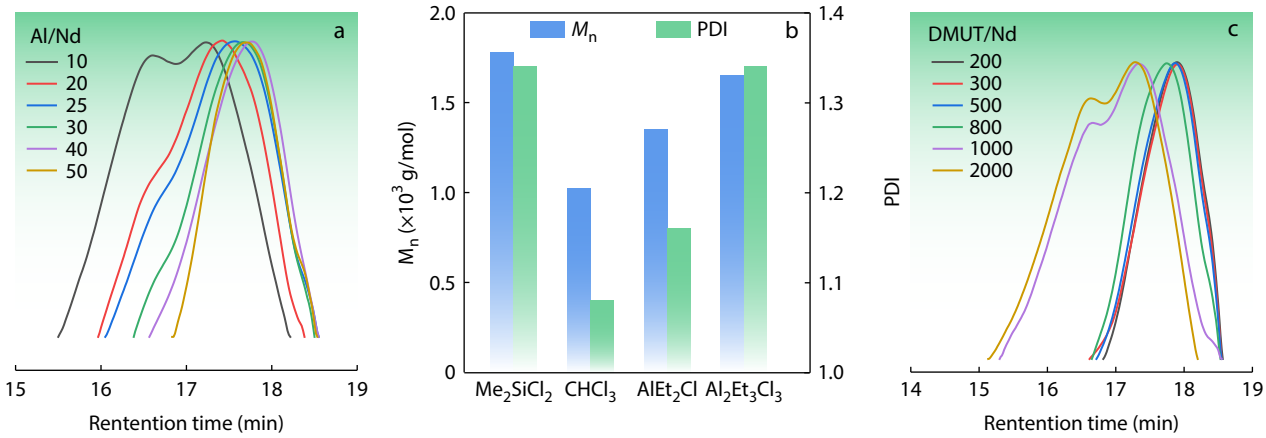

Fig. 2 (a) GPC curves of PDMUT obtained from Table 1; (b) M_n and PDI of products under different types of chlorides; (c) GPC curves of polymerization obtained from Table 2.

Table 2 Nd-promoted DMUT polymerization under different [DMUT]/[Nd] ratios.

Run	[DMUT]/[Nd] (mol/mol)	Yield (%)	M_n [a] ($\times10^3$)	M_w [a] ($\times10^3$)	PDI	Microstructure [b] (%)	
						1,4-	1,2-
1	200	44.5	1.49	1.90	1.28	29.53	70.47
2	300	48.9	1.52	1.99	1.31	28.61	71.39
3	500	53.2	1.78	2.39	1.34	27.47	72.53
4	800	59.6	1.78	2.33	1.33	26.23	73.77
5	1000	80.5	3.51	7.49	2.13	25.03	74.97
6	2000	78.6	4.24	8.82	2.08	24.84	75.16

Polymerization conditions: [M]=1.85 mol/L, in hexane, 50 °C, 24 h. [DIBAH]/[Nd]=40, Cl/Nd=3.0 (Me_2SiCl_2). [a] Determined by GPC, using polystyrene as standard. [b] Determined by NMR.

monomer, which restricts chain propagation at the Nd active site. Additionally, it seems that the gradually broadened polydispersities are accompanied by increased molecular weights. This phenomenon was likely associated with the increased viscosity of the system, which rendered the reversible chain transfer to DIBAH irreversible.

Structure of the Obtained PDMUT

Using the Nd-based catalytic system, DMUT undergoes polymerization predominantly *via* 1,4- and 1,2- manners (Fig. 3a), as revealed by the FTIR spectrum of PDMUT (Fig. 3b), in which bands at 738 and 968 cm^{-1}, which indicate the *cis*-1,4-/1,2- and *trans*-1,4-/1,2- structures, respectively, were clearly observed. No 3,4- units with a typical band at 911 cm^{-1} was detected. The representative ^{1}H-NMR spectrum of the resulting PDMUT is shown in Fig. 3(c). The broad peak in the range of 5.15–5.38 ppm were attributed to the protons of H2 in the 1,4-inserted unit, as well as the protons of H4′ in the 1,2-inserted units; the peak at 4.76–5.15 ppm corresponds to the protons of H3/H3′ and H9/H9′. In the spectrum, a distinctive peak solely observed in the 1,4-inserted unit was observed at 2.41 ppm, assigned to the methine proton H4 adjacent to the double bond. The broad peak spanning 1.75–2.20 ppm was assigned to the allylic protons, including H1, H8, H2′, H5′ and H8′. Terminal methyl proton of PDMUT unit appear at 1.66 and 1.59 ppm respectively, corresponding to H11/H11′ and H10/H10′ respectively. As a broad peak, protons of H12/H12′ were observed at 0.73–0.94 ppm. The remaining protons were observed at 0.93–1.49 ppm, because of their extensive overlapping, detailed assignments could not be determined. The position of the hydrogen in the polymer was also confirmed by HH-COSY NMR spectroscopy (Fig. 3d).

Based on the above assignments, the percentage of 1,4-inserted units (*A*) can be determined using the following equation:

$$A = \frac{5 \times I_{2.41}}{I_{1.75-2.20} + I_{2.41}} \quad (1)$$

where in $I_{2.41}$ is the integral area of proton H_4, and $I_{1.75-2.20}$ is the integral area of protons H1, H8, H2′, H5′ and H8′ (for detailed steps of the equation derivation, please refer to page S(2) in the ESI).

The microstructures of the obtained PDMUTs can be determined according to Eq. (1), and the results are summarized in Tables 1–2. The data indicated that the microstructure of the PDMUTs was strongly influenced by the [DIBAH]/[Nd] and [DMUT]/[Nd] ratios. Specifically, a higher cocatalyst concentration resulted in products with higher 1,4-contents and correspondingly lower 1,2-contents. For instance, increasing the [DIBAH]/[Nd] ratio from 10 to 50 increased the 1,4-content of the PDMUTs from 17.95% to 28.08%, while the 1,2-content decreased from 82.05% to 71.92%. Conversely, increasing the [DMUT]/[Nd] ratio from 200 to 2000 (effectively reducing the precatalyst concentration) produced PDMUTs with progressively lower 1,4-contents, decreasing from 29.53% to 24.84%, while the 1,2-contents increased from 70.47% to 75.16%. Despite these variations, all PDMUT products predominantly exhibited a 1,2-structure (70%–80%), in contrast to the high *cis*-1,4-selectivity typically reported for Nd-based catalytic systems with other conjugated diene monomers, such as 1,3-butadiene, isoprene, and myrcene.[53] This deviation likely arises

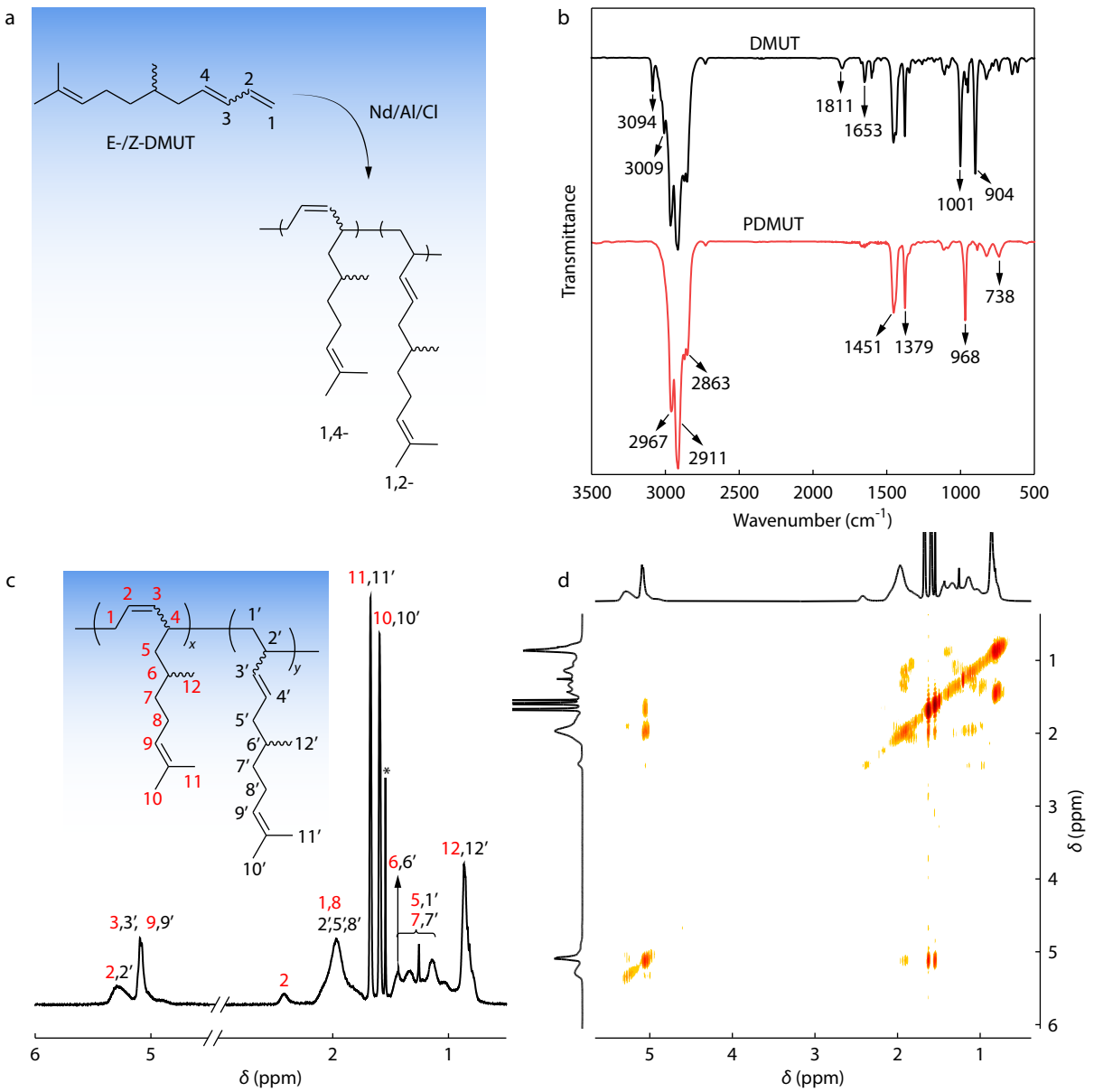

Fig. 3 (a) Polymerization of *E*-/*Z*- DMUT; (b) FTIR spectra of DMUT monomer and PDMUT from Table 2, entry 5; (c) ^{1}H-NMR spectrum of PDMUT obtained from Table 2, entry 5, (* denotes chemical shift of water); (d) COSY (400MHz, $CDCl_3$) spectrum of PDMUT from Table 2, entry 5.

from steric hindrance introduced by the two methyl-substituted side chains of the DMUT monomer, which disfavors the 1,4-insertion pathway and promotes 1,2-regioselectivity.

The ^{13}C-NMR spectrum of PDMUT is shown in Fig. 4(A), with signal assignments based on chemical shift values, DEPT 135, and ^{1}H-^{13}C 2D NMR spectroscopy (Figs. 4B and 4C). In the olefinic carbon region, signals at 126.66–129.48 ppm are assigned to carbons Cb/Cd′, which correlate with protons of H2/H4′ (5.15–5.38 ppm) in the HSQC spectrum. Carbon Cc/Cc′ appeared at 134.91–137.52 ppm, which also shows clear correlation with H3/H3′ at 4.76–5.15 ppm in the HSQC spectrum. Pendant carbons Cj/Cj′ and Ck/Ck were identified at 124.88–125.63 ppm and 130.55–131.35 ppm. The absence of Ck/Ck′ signals in the DEPT 135 spectrum confirms their quaternary nature. In the HSQC spectrum, carbon Cj/Cj′ correlates with protons H9/H9′, and in the HMBC spectrum, both carbons Cj/Cj′ and Ck/Ck′ clearly correlate with H11/H11′ and H10/H10′, respectively. In the aliphatic carbon region, methyl carbons Cm/Cm′ and Cl/Cl′ are easily identified at 17.80 ppm and 25.92 ppm respectively, because they show obvious correlation with H10/H10′ and H11/H11′ in the HSQC spectrum and H9/H9′ in the HMBC spectrum. Another set of methyl carbons Cg/Cg′ are observed in the range of 18.77–20.66 ppm, and their correlation with H9/H9′ in the HSQC spectrum can be also obviously observed. The remaining resonance assignments are shown in Fig. 4(A), from which the predominant 1,2-structure of PDMUT was confirmed. For instance, the resonance peak at 40.25 ppm that was assigned to Ca′ in the 1,2-structure, exhibited a significantly higher intensity than the peak of Ca (33.87–34.95 ppm) in the 1,4-structure.

In addition to the polymer microstructure, the chain structure of the polymer was characterized using matrix-assisted

https://doi.org/10.1007/s10118-025-3408-5

laser desorption ionization-time of flight (MALDI-TOF) spectroscopy. As shown in Fig. 5, one major peak (blue) and two minor peaks (yellow and red) were clearly detected. The blue peak corresponds to the structure of DMUT (178.32) × *n* + Ag^+ (107.87), and the yellow and red peaks correspond to the structures of DMUT (178.32) × *n* + Ag^+ (107.87) + H_2O (18.02) and DMUT (178.32) × *n* + K^+ (39.08) + H_2O (18.02), respectively. This result indicates that the PDMUT chain is capped with two hydrogen atoms on the *α*- and *ω*-ends, wherein *α*-end hydrogen atom is derived from the cocatalyst DIBAH (Al(*i*-Bu)$_2$H) and the *ω*-end hydrogen atom comes from ethanol or acidified water, which is used to quench the polymerization.

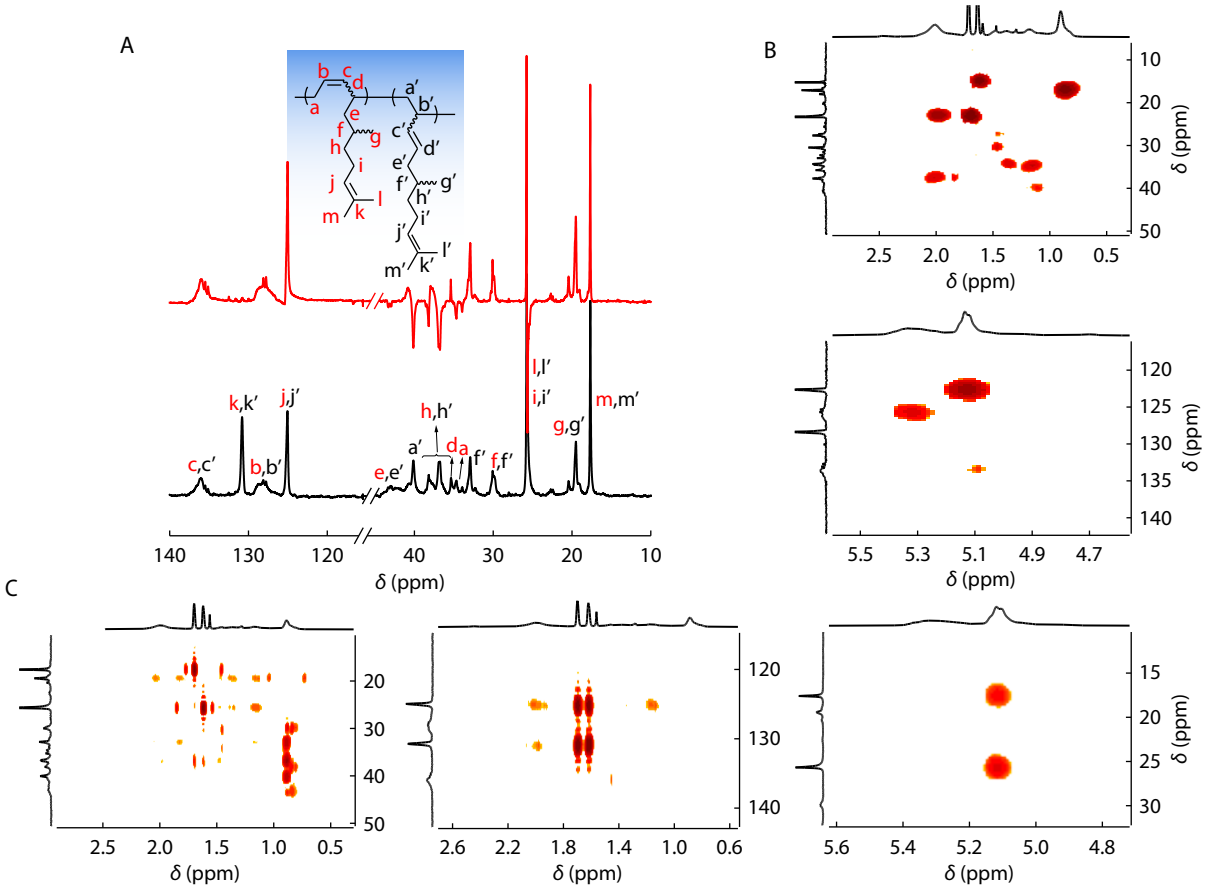

Fig. 4 (A) ^{13}C-NMR and DEPT 135 spectra, (B) HSQC, and (C) HMBC of PDMUT obtained from Table 3, entry 5.

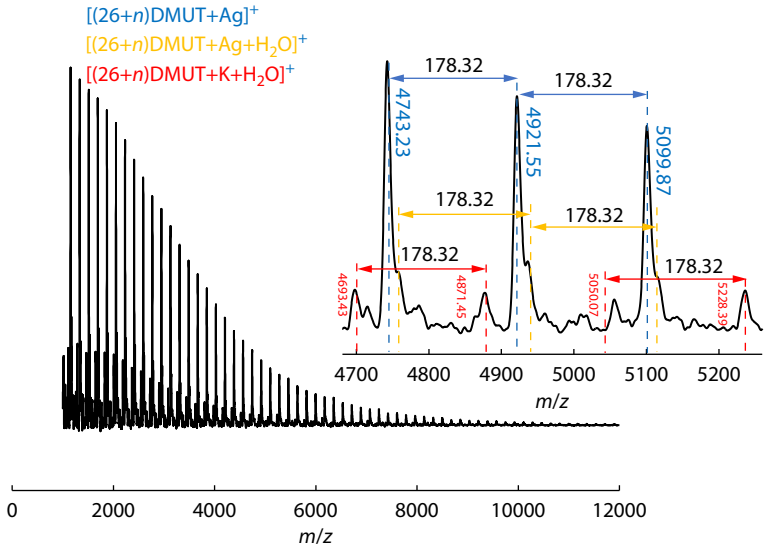

Fig. 5 MALDI-TOF spectrum of the obtained PDMUT in Table 3 (run5).

https://doi.org/10.1007/s10118-025-3408-5

Thermal Analysis of the Obtained PDMUT

The glass transition temperature (T_g) of the obtained PDMUT was measured using DSC, and the curve is presented in Fig. 6(A). For comparison, the DSC curves of polymyrcene (PMy) and polyisoprene (PIP) were also included. Both PMy (1,4-microstructure: 92.59%, molecular weight: 12.9×10^3 Dalton) and PIP (1,4-microstructure: 95.36%, molecular weight: 2.9×10^3 Dalton) were prepared using the same NdV/DIBAH/Me_2SiCl_2 catalytic system under similar conditions. It was found that, PDMUT exhibited a relative higher T_g of –55.1 °C, which is 12.3 °C and 13.6 °C higher than that of PMy and PIP, respectively. This result suggests that PDMUT possesses a more rigid polymer chain than those of PMy and PIP. The increased rigidity is attributed to PDMUT's higher 1,2-content of PDMUT, in contrast to the higher 1,4-content of PMy and PIP, as a higher 1,4-structure typically results in greater chain flexibility.

The thermal stabilities of the PDMUT, PMy, and PIP were also compared. As shown in Fig. 6(B), PDMUT shows an initial degradation at 187.62 °C and its weight slowly decreased by 15 wt% until a second dramatic degradation occurred at 412.04 °C. This trend showed striking contrast to PMy and PIP, whose degradation occurred at a similar temperature of 396.04 °C. After 396.04 °C, PIp degraded slightly faster than PDMUT and PMy, which degraded at a similar rate, perhaps because of their similar pendant groups.

Hydrogenation and Thermal Behavior of PDMUT

Hydrogenated polydiene rubber products typically exhibit superior thermal and chemical resistance compared with their non-hydrogenated counterparts, thereby broadening their potential applications. To enhance these properties, PDMUT was subjected to hydrogenation using *p*-toluenesulfonylhydrazide (TSH) as a hydrogenation agent. Under reflux in xylene with excess TSH, PDMUT can be converted into fully hydrogenated PDMUT (HPDMUT) as the expected product. ^{1}H-NMR spectrum of the obtained HPDMUT (Fig. 6C) confirmed complete hydrogenation, as evidenced by the disappearance of the olefinic proton signals (4.76–5.38 ppm), indicating full saturation of the double bonds. The newly appeared tertiary hydrogens H10′ locates in the range of 1.47–1.58 ppm, and methyl protons of H11/H11′, H12/H12′ and H13/H13′ resonate at 0.86, 0.88, 0.81–0.84 ppm respectively. The other protons appeared in the

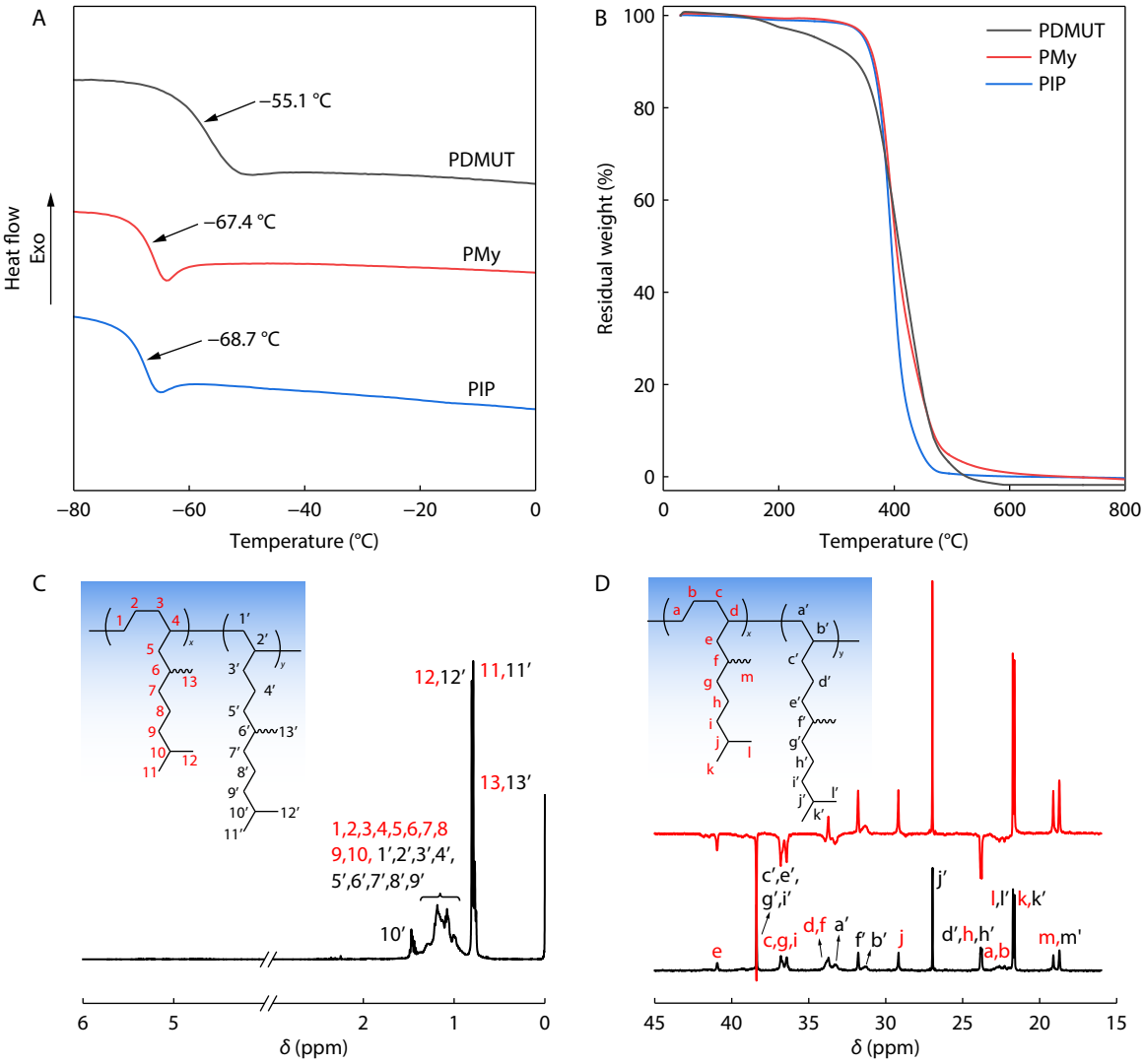

Fig. 6 (A) DSC thermograms and (B) TGA thermograms of PDMUT, PMy, PIP; (C) ^{1}H-NMR, (D) ^{13}C-NMR and DEPT 135 spectra of HPDMUT.

https://doi.org/10.1007/s10118-025-3408-5

region of 0.88–1.39 ppm, and severe overlapping occurred, which prevented further exact assignments. The ^{13}C and ^{1}H-^{13}C HSQC NMR spectra of HPDMUT and their corresponding signal assignments are shown in Fig. 6(D), wherein carbon C10′ can be readily identified because of its correlation with H10′ in the HSQC spectrum. Methyl carbons Ck/Ck′, Cl/Cl′ and Cm/Cm′ appear at 21.64, 21.74, 18.54–19.25 ppm respectively, with clear correlations to their corresponding protons of H11/H11′, H12/H12′ and H13/H13′ in the HSQC spectrum (Fig. S1 in ESI). Regarding the thermal properties, HPDMUT exhibits a slightly higher T_g (–51.1 °C) compared to PDMUT, likely due to increased main-chain rigidity after being hydrogenation (Fig. S2 in ESI).

Copolymerization of DMUT with Isoprene (IP) and Butadiene (BD)

To further explore the compositional flexibility and application potential of DMUT-based materials, we investigated their copolymerization with two classical conjugated dienes: IP and BD. Copolymerization with IP was conducted under the same Nd-based catalytic conditions as those used for homopolymerization. As shown in Table 3, the reactions proceeded efficiently, yielding copolymers with moderate to high conversions (42.5%–76.6%) depending on the DMUT/IP feeding ratio. Notably, all the samples exhibited unimodal GPC curves (Fig. 7a), indicating true copolymer formation rather than a mixture of homopolymers, suggesting initiation from a unified catalytic species.

The successful incorporation of IP segments was confirmed by the emergence of characteristic ^{1}H-NMR peaks at 4.75 ppm (3,4-IP), and sharper signals at 5.12 ppm (1,4-IP methine) and 2.02 ppm (1,4-IP methylene) (Fig. 7b), which were absent in the spectrum of pure PDMUT in Fig. 3(c). As the IP feeding ratio increased, these signals intensified proportionally, confirming the tunability of copolymer composition. Quantitative analysis from ^{1}H-NMR further revealed that IP was incorporated more efficiently than its initial feeding ratio, indicating its higher polymerization activity compared to that of DMUT. To quantify this observation, the reactivity ratios of IP (r_{IP}) and DMUT (r_{DMUT}) were calculated using the Fineman–Ross formula, as follows:[54]

$$[(1 - f)/f]F = r_{IP} - r_{DMUT}F^2/f \quad (2)$$

where F and f denote the molar ratio of IP to DMUT in the feed and in the resulting copolymer, respectively, as determined by ^{1}H-NMR spectra. The calculated reactivity ratios, as shown in Table S2 and Fig. S3 (in ESI), were r_{IP}=1.38 and r_{DMUT}=0.24, respectively. These values clearly indicate that IP is significantly more active than DMUT, which is likely attributable to the lower steric hindrance of IP. In addition, the thermal properties of the obtained DMUT/IP copolymers were investigated. As shown in Fig. S4 (in ESI), the T_g of the copolymers gradually increased with increasing DMUT content, ranging from –67.7 °C to –64.3 °C. This trend supports the hypothesis that incorporating bulkier DMUT units restricts segmental mobility, enabling the precise tuning of the copolymers' thermal properties by adjusting the DMUT/IP ratio. The thermal and structural tunability of DMUT-based homopolymers and copolymers make them promising candidates for use as processing aids in rubber compounding, wherein key performance parameters, such as mobility, low-temperature properties, and antioxidative characteristics, can be precisely tailored to meet application requirements. Moreover, these copolymers were derived from a green monomer of DMUT, enhancing their appeal for applications where sustainable rubber additives are essential.

Copolymerization with BD followed similar trends (Table S3 in ESI, Fig. 7c). Higher BD feed ratios resulted in increased yields (up to 73.8%) and reduced DMUT incorporation, as confirmed by ^{1}H-NMR spectroscopy (Fig. 7d). BD also showed higher activity than DMUT, which is consistent with its smaller molecular size and greater accessibility to the catalytic site. Taken together, these results demonstrate that DMUT not only undergoes efficient homopolymerization, but also copolymerizes readily with traditional diene monomers. Incorporation of bulky, branched DMUT segments into IP and BD backbones enables the preparation of polydiene copolymers with tunable compositions and microstructures. This structural integration is expected to modulate the key thermal and mechanical properties, potentially affording new elastomeric materials with enhanced rigidity and adjustable glass transition temperatures.

CONCLUSIONS

In summary, the present study presents a new and facile strategy for converting bio-based citronellal into a polydiene polymer of poly(6,10-dimethyl-1,3,9-undecatriene) (PDMUT). In the Wittig reaction, citronellal is first converted to dienic DMUT, which subsequently undergoes polymerization using an Nd-based coordination catalytic system. The structures of the DMUT monomer and the PDMUT products were fully characterized. By varying the polymerization conditions, such as the DIBAH/Nd ratio, chloride donor type, and DMUT/Nd ratio, *etc.*, PDMUT products with different molecular weights, polydispersities, and microstructures can be achieved. As evidenced by ^{1}H, ^{13}C, HSQC, and HMBC NMR analyses, the resultant PDMUT predominantly exhibited a 1,2-content. The thermal properties of PDMUT were also investigated by DSC and TGA, and their differences from other common polydiene-based polymers were compared. Furthermore, the copolymerization of DMUT with isoprene and 1,3-

Table 3 Copolymerization of DMUT and IP at different [DMUT]/[IP]/[Nd] ratios.[a]

Entry	[DMUT]/([IP] or [BD])	Yield (%)	M_n[b] ($\times 10^3$)	PDI[b]	Content[c] (%)	
					PDMUT	PI
1	400:100	42.5	9.4	1.96	77.5	22.5
2	300:200	55.4	7.7	1.89	58.8	41.2
3	200:300	67.9	7.6	1.84	40.9	59.1
4	100:400	76.6	7.0	1.83	31.2	68.8

[a] Polymerization conditions: [DMUT+IP] = 1.85 mol/L, in hexane, 50 °C, 24 h, [M]/[Nd] = 500, [DIBAH]/[Nd] = 40, [Cl]/[Nd] = 3.0 (Me_2SiCl_2), catalyst feeding order: Nd + (DMUT + IP) + DIBAH + Cl. [b] Determined by GPC using polystyrene standards. [c] Determined by ^{1}H-NMR.

https://doi.org/10.1007/s10118-025-3408-5

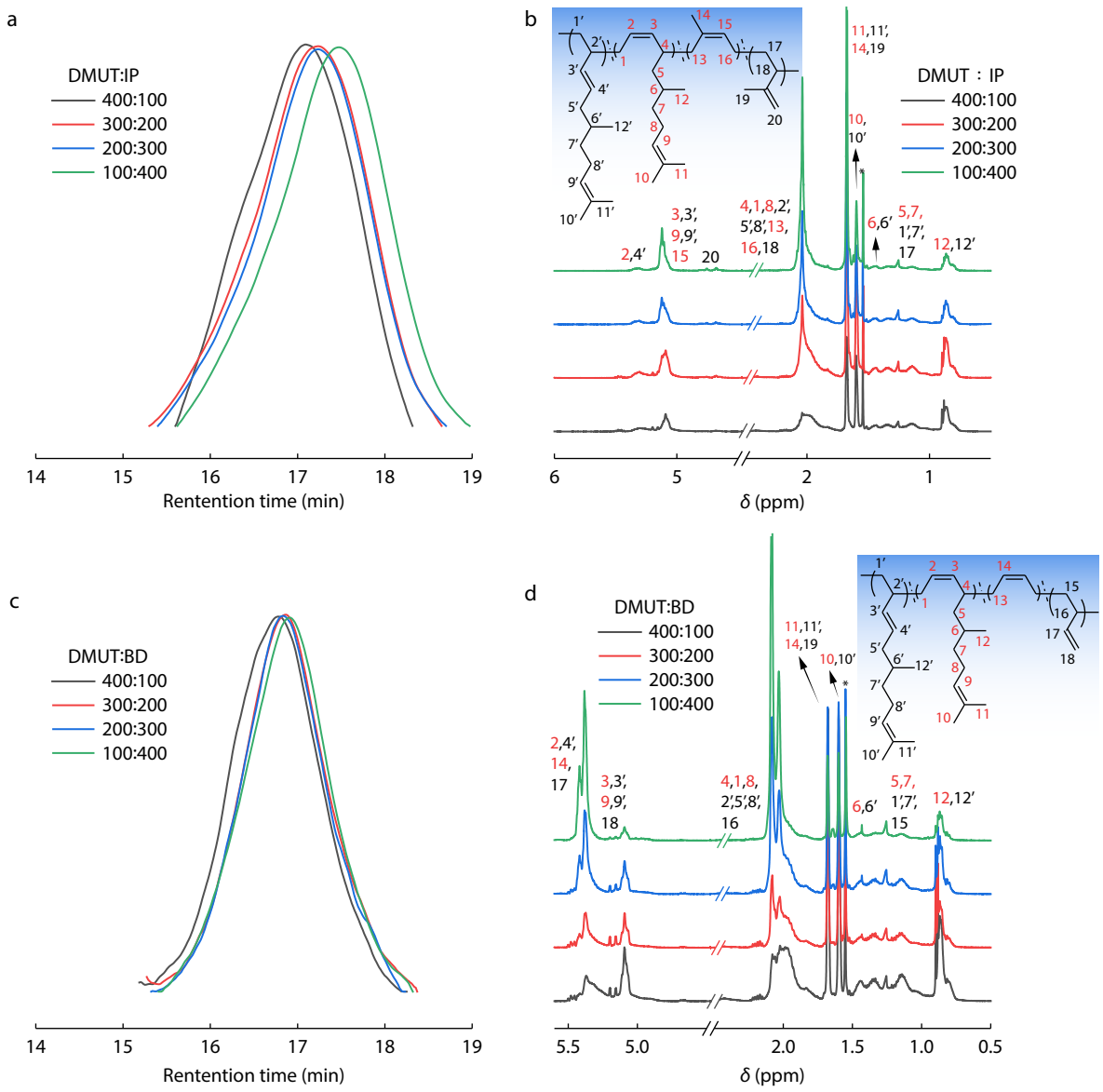

Fig. 7 (a) GPC curves obtained from Table 3; (b) ^{1}H-NMR spectra of DMUT/IP copolymers; (c) GPC curves obtained from Table 3; (d) ^{1}H-NMR spectra of DMUT/BD copolymers.

butadiene was successfully achieved, affording unimodal copolymers with adjustable compositions and potential for tailored performance. These findings highlight the versatility of DMUT as a bio-based monomer and provide a new avenue for the design of sustainable polydiene elastomers with customizable thermal and mechanical properties.

Conflict of Interests

The authors declare no interest conflict.

Electronic Supplementary Information

Electronic supplementary information (ESI) is available free of charge in the online version of this article at http://doi.org/10.1007/s10118-025-3408-5.

Data Availability Statement

Data will be made available on request.

ACKNOWLEDGMENTS

This work was financially supported by the National Key R&D Program of China (No. 2022YFC2104702) and the National Natural Science Foundation of China (No. 22071236). H.L. thanks for the financial support from the Taishan Scholars Program (No. tsqn202211165).

REFERENCES

1 Wang, Z.; Ganewatta, M. S.; Tang, C. Sustainable polymers from biomass: bidging chemistry with materials and processing. *Prog. Polym. Sci.* **2020**, *101*, 101197.

2 Liu, J.; Wang, S.; Peng, Y.; Zhu, J.; Zhao, W.; Liu, X. Advances in sustainable thermosetting resins: From renewable feedstock to high performance and recyclability. *Prog. Polym. Sci.* **2021**, *113*, 101353.
3 Rosenboom, J. G.; Langer, R.; Traverso, G. Bioplastics for a circular economy. *Nat. Rev. Mater.* **2022**, *7*, 117–137.
4 Ganewatta, M. S.; Wang, Z.; Tang, C. Chemical syntheses of bioinspired and biomimetic polymers toward biobased materials. *Nat. Rev. Chem.* **2021**, *5*, 753–772.
5 Lamparelli, D. H.; Winnacker, M.; Capacchione, C. Stereoregular polymerization of acyclic terpenes. *ChemPlusChem* **2022**, *87*, e202100366.
6 Bakkali, F.; Averbeck, S.; Averbeck, D.; Idaomar, M. Biological effects of essential oils—a review. *Food Chem. Toxicol.* **2008**, *46*, 446–475.
7 Wahlen, C.; Frey, H. Anionic polymerization of terpene monomers: new options for bio-based thermoplastic elastomers. *Macromolecules* **2021**, *54*, 7323–7336.
8 Zhao, J.; Schlaad, H., Synthesis of terpene-based polymers. In *bio-synthetic polymer conjugates*, Schlaad, H., Ed. Springer Berlin Heidelberg: Berlin, Heidelberg, **2013**, pp. 151–190.
9 Winnacker, M. Terpene-based polyamides: a sustainable polymer class with huge potential. *Curr. Opin. Green Sust.* **2023**, *41*, 100819.
10 Kamigaito, M.; Satoh, K., Sustainable vinyl polymers via controlled polymerization of terpenes. In *Sustainable Polymers from Biomass*, **2017**, pp. 55–90.
11 Zhu, Y.; Romain, C.; Williams, C. K. Sustainable polymers from renewable resources. *Nature* **2016**, *540*, 354–362.
12 Georges, S.; Bria, M.; Zinck, P.; Visseaux, M. Polymyrcene microstructure revisited from precise high-field nuclear magnetic resonance analysis. *Polymer* **2024**, *55*, 3869–3878.
13 Loughmari, S.; Hafid, A.; Bouazza, A.; El Bouadili, A.; Zinck, P.; Visseaux, M. Highly stereoselective coordination polymerization of β-myrcene from a lanthanide-based catalyst: access to bio-sourced elastomers. *J. Polym. Sci. Polym. Chem.* **2012**, *50*, 2898–2905.
14 Liu, B.; Li, L.; Sun, G.; Liu, D.; Li, S.; Cui, D. Isoselective 3,4-(co)polymerization of bio-renewable myrcene using NSN-ligated rare-earth metal precursor: an approach to a new elastomer. *Chem. Commun.* **2015**, *51*, 1039–1041.
15 Liu, B.; Liu, D.; Li, S.; Sun, G.; Cui, D. High trans-1,4 (co)polymerization of *β*-myrcene and isoprene with an iminophosphonamide lanthanum catalyst. *Chinese J. Polym. Sci.* **2016**, *34*, 104–110.
16 Métafiot, A.; Kanawati, Y.; Gérard, J.-F.; Defoort, B.; Marić, M. Synthesis of *β*-myrcene-based polymers and styrene block and statistical copolymers by SG1 nitroxide-mediated controlled radical plymerization. *Macromolecules* **2017**, *50*, 3101–3120.
17 Jia, X.; Li, W.; Zhao, J.; Yi, F.; Luo, Y.; Gong, D. Dual catalysis of the selective polymerization of biosourced myrcene and methyl methacrylate promoted by salicylaldiminato cobalt(II) complexes with a pendant donor. *Organometallics* **2018**, *38*, 278–288.
18 Ren, X.; Guo, F.; Fu, H.; Song, Y.; Li, Y.; Hou, Z. Scandium-catalyzed copolymerization of myrcene with ethylene and propylene: convenient syntheses of versatile functionalized polyolefins. *Polym. Chem.* **2018**, *9*, 1223–1233.
19 Li, W.; Zhao, J.; Zhang, X.; Gong, D. Capability of PN3-type cobalt complexes toward selective (co-)polymerization of myrcene, butadiene, and isoprene: access to biosourced polymers. *Ind. Eng. Chem. Res.* **2019**, *58*, 2792–2800.
20 Yu, X.; Li, M.; Hong, J.; Zhou, X.; Zhang, L. Living 3,4-(co)polymerization of isoprene/myrcene and one-pot synthesis of a polyisoprene blend catalyzed by binuclear rare-earth metal amidinate complexes. *Chem. Eur. J.* **2019**, *25*, 2569–2576.
21 Xu, Y.; Zhao, J.; Gan, Q.; Ying, W.; Hu, Z.; Tang, F.; Luo, W.; Luo, Y.; Jian, Z.; Gong, D. Synthesis and properties investigation of hydroxyl functionalized polyisoprene prepared by cobalt catalyzed co-polymerization of isoprene and hydroxylmyrcene. *Polym. Chem*. **2020**, *11*, 2034–2043.
22 Kitphaitun, S.; Chaimongkolkunasin, S.; Manit, J.; Makino, R.; Kadota, J.; Hirano, H.; Nomura, K. Ethylene/myrcene copolymers as new bio-based elastomers prepared by coordination polymerization using titanium catalysts. *Macromolecules* **2021**, *54*, 10049–10058.
23 Wang, Q. Y.; Sang, L. P.; Zhang, Z.; Jiang, Y.; Tian, H.; Zhao, X.; Guo, X.; Li, S.-H. Regio- and stereoselective polymerization of bio-based ocimene by rare-earth metal catalysts. *Chinese J. Polym. Sci.* **2024**, *42*, 223–229.
24 Wadgaonkar, S. P.; Wagner, M.; Baptista, L. A.; Cortes-Huerto, R.; Frey, H.; Müller, A. H. E. Anionic polymerization of the terpene-based diene β-ocimene: complex mechanism due to stereoisomer reactivities. *Macromolecules* **2023**, *56*, 664–677.
25 Radchenko, A. V.; Bouchekif, H.; Peruch, F. Triflate esters as in-situ generated initiating system for carbocationic polymerization of vinyl ethers, isoprene, myrcene and ocimene. *Eur. Polym. J.* **2017**, *89*, 34–41.
26 Peng, D.; Du, G.; Zhang, P.; Yao, B.; Li, X.; Zhang, S. Regio- and stereochemical control in ocimene polymerization by half-sandwich rare-earth metal dialkyl complexes. *Macromol. Rapid Commun.* **2016**, *37*, 987–992.
27 Naddeo, M.; Buonerba, A.; Luciano, E.; Grassi, A.; Proto, A.; Capacchione, C. Stereoselective polymerization of biosourced terpenes *β*-myrcene and *β*-ocimene and their copolymerization with styrene promoted by titanium catalysts. *Polymer* **2017**, *131*, 151–159.
28 Lamparelli, D. H.; Paradiso, V.; Monica, F. D.; Proto, A.; Guerra, S.; Giannini, L.; Capacchione, C. Toward more sustainable elastomers: stereoselective copolymerization of linear terpenes with butadiene. *Macromolecules* **2020**, *53*, 1665–1678.
29 Sahu, P.; Bhowmick, A. K. Redox emulsion polymerization of terpenes: mapping the effect of the system, structure, and reactivity. *Ind. Eng. Chem. Res.* **2019**, *58*, 20946–20960.
30 Lamparelli, D. H.; Paradiso, V.; Capacchione, C. New elastomeric materials from biomass: stereoselective polymerization of linear terpenes and their copolymerization with butadiene by using a cobalt complex with phosphane ligands. *Rub. Chem. Technol.* **2020**, *93*, 605–614.
31 Luk, S. B.; Maríc, M. Polymerization of biobased farnesene in miniemulsions by nitroxide-mediated polymerization. *ACS Omega* **2021**, *6*, 4939–4949.
32 You, F.; Kang, X.; Nishiura, M.; Zhai, J.; Xu, S.; Wang, J.; Shi, X.; Hou, Z. Living 3,4-isoselective (co)polymerization of biobased β-farnesene catalyzed by phosphine-functionalized fluorenyl rare-earth metal catalysts. *Macromolecules* **2022**, *55*, 5049–5057.
33 Luk, S. B.; Maric, M. Farnesene and norbornenyl methacrylate block copolymers: application of thiol-ene clicking to improve thermal and mechanical properties. *Polymer* **2021**, *230*, 124106.
34 Jiang, Y.; Zhang, Z.; Li, S.; Cui, D. Coordination polymerization of renewable (E)-4,8-dimethyl-1,3,7-nonatriene by rare-earth metal catalysts. *Chin. J. Chem.* **2022**, *40*, 1939–1944.
35 Sahu, P.; Sarkar, P.; Bhowmick, A. K. Synthesis and characterization of a terpene-based sustainable polymer: poly-alloocimene. *ACS Sustain. Chem. Eng.* **2017**, *5*, 7659–7669.
36 Jones, J. F. Cyclopolymerization. III. poly-alloocimene. *J. Polym. Sci.* **1958**, *33*, 513–515.
37 Puskas, J. E.; Gergely, A. L.; Kaszas, G. Controlled/living carbocationic copolymerization of isobutylene with alloocimene. *J. Polym. Sci. Polym. Chem.* **2013**, *51*, 29–33.
38 Gergely, A. L.; Puskas, J. E. Synthesis and characterization of

https://doi.org/10.1007/s10118-025-3408-5

thermoplastic elastomers with polyisobutylene and polyalloocimene blocks. *J. Polym. Sci. Polym. Chem.* **2015**, *53*, 1567–1574.
39 Venancio, A. N.; Silva, M. J.; Parreira, L. A.; Júlio, A. A.; Souza, G. R.; Conceição Santos, M. F.; Menini, L. Citronellall: a natural aldehyde with important properties. *Nat. Prod. Res.* **2025**, *39*, 1199–1212.
40 Rokonuzzman, M.; Bhuia, M. S.; Al-Qaaneh, A. M.; El-Nashar, H. A. S.; Islam, T.; Chowdhury, R.; Hasan Shanto, H.; Al Hasan, M. S.; El-Shazly, M.; Torequl Islam, M. Biomedical perspectives of citronellall: biological activities, toxicological profile and molecular mechanisms. *Chem. Biodivers.* **2025**, *22*, 202401973.
41 Mäki-Arvela, P.; Simakova, I.; Vajglová, Z.; Murzin, D. Y. One-pot synthesis of menthol from citral and citronellall over heterogeneous catalysts. *Catal. Surv. Asia* **2023**, *27*, 2–19.
42 Ricci, G.; Zetta, L.; Porri, L.; Meille, S. V. Synthesis and characterization of isotactic cis-1,4-poly(3-methyl-1,3-pentadiene). *Macromol. Chem. Phys.* **1995**, *196*, 2785–2793.
43 Hu, Y.; Dong, W.; Masuda, T. Novel methylaluminoxane-activated neodymium isopropoxide catalysts for 1,3-butadiene polymerization and 1,3-butadiene/isoprene copolymerization. *Macromol. Chem. Phys.* **2013**, *214*, 2172–2180.
44 Wang, F.; Liu, H.; Hu, Y.; Zhang, X. Lanthanide complexes mediated coordinative chain transfer polymerization of conjugated dienes. *Sci. China Technol. Sci.* **2018**, *61*, 1286–1294.
45 Leone, G.; Caterina Boccia, A.; Ricci, G.; Giarrusso, A.; Porri, L. Polymerization of (E)-1,3-pentadiene and (E)-2-methyl-1,3-pentadiene with neodymium catalysts: examination of the factors that affect the stereoselectivity. *J. Polym. Sci. Polym. Chem.* **2013**, *51*, 3227–3232.
46 Ricci, G.; Boccia, A. C.; Palucci, B.; Sommazzi, A.; Masi, F.; Scoti, M.; De Stefano, F.; De Rosa, C. Synthesis of stereoregular polymyrcenes using neodymium-, iron- and copper-based catalysts. *Polym. Chem.* **2024**, *15*, 1367–1376.
47 Gan, Q.; Xu, Y.; Huang, W.; Luo, W.; Hu, Z.; Tang, F.; Jia, X.; Gong, D. Utilization of bio-sourced myrcene for efficient preparation of highly cis-1,4 regular elastomer *via* a neodymium catalyzed copolymerization strategy. *Polym. Int.* **2020**, *69*, 763–770.
48 Wang, F.; Zhang, C.; Hu, Y.; Jia, X.; Bai, C.; Zhang, X. Reversible coordinative chain transfer polymerization of isoprene and copolymerization with ε-caprolactone by neodymium-based catalyst. *Polymer* **2012**, *53*, 6027–6032.
49 Cheng, L.; Li, M. M.; Xiao, L. J.; Xie, J. H.; Zhou, Q. L. Nickel(0)-catalyzed hydroalkylation of 1,3-dienes with simple ketones. *J. Am. Chem. Soc.* **2018**, *140*, 11627–11630.
50 Timsina, Y. N.; Biswas, S.; RajanBabu, T. V. Chemoselective reactions of (E)-1,3-dienes: cobalt-mediated isomerization to (*Z*)-1,3-dienes and reactions with ethylene. *J. Am. Chem. Soc.* **2014**, *136*, 6215–6218.
51 Friebe, L.; Windisch, H.; Nuyken, O.; Obrecht, W. Polymerization of 1,3-butadiene initiated by neodymium versatate/triisobutylaluminum/ethylaluminum sesquichloride: impact of the alkylaluminum cocatalyst component. *J. Macromol. Sci. Pur.* **2004,** *A41*, 245–256.
52 Wang, F.; Liu, H.; Zheng, W.; Guo, J.; Zhang, C.; Zhao, L.; Zhang, H.; Hu, Y.; Bai, C.; Zhang, X. Fully-reversible and semi-reversible coordinative chain transfer polymerizations of 1,3-butadiene with neodymium-based catalytic systems. *Polymer* **2013**, *54*, 6716–6724.
53 Friebe, L.; Nuyken, O.; Obrecht, W. in *Neodymium-based Ziegler/Natta catalysts and their application in diene polymerization*. Springer-Verlag Berlin Heidelbery, **2006**, pp. 9–12.
54 Liu, X.; Zheng, H.; Wang, X.; Jiang, Z.; Gu, J.; Liu, H.; Zhang, C.; Yang, Q.; Zhang, X. Novel butadiene/isoprene copolymer with predominant 1,2/3,4-units: a tough thermoplastic elastomer material with superior dynamic mechanical properties. *Eur. Polym. J.* **2023**, *196*, 112333.

https://doi.org/10.1007/s10118-025-3408-5